Performance Analysis for Flexible Pavements with Stabilized Base

M. C. WANG

The performance of experimental pavements at the Pennsylvania Transportation Research Facility was evaluated. These pavements contained five different types of base course: bituminous concrete, aggregate bituminous, aggregate cement, aggregate-lime-pozzolan, and crushed stone. Most of the pavements had been subjected to about 2.4 million 18-kip equivalent axle loads (EALs), which is equivalent to approximately 40-years service life. Data analyzed were pavement serviceability index and three distress manifestations--roughness, rutting, and cracking. Some existing pavement performance models were also evaluated by using the performance data. The performance data indicate that the trend of serviceability index loss with increasing EAL follows the power function developed at the American Association of State Highway Officials (AASHO) Road Test. Of the performance models evaluated--AASHO, modified Highway Research Board (HRB), and Painter's models--the AASHO model appears to predict best, although it overpredicts pavement service life. By using a curve-fitting process and regression analysis, equations that relate pavement performance indicators and structural number are formulated. These equations permit prediction of the rate of serviceability loss and pavement life required to reach a certain present serviceability index drop. Also developed are equations that relate distress with structural number and critical pavement response with pavement service life. These equations may be used to predict various distress intensities from structural numbers and also used to predict pavement life from critical response. According to the results of the analysis, the maximum compressive strain at the top of the subgrade appears to be a better factor than the maximum surface deflection for predicting pavement service life.

The American Association of State Highway Officials (AASHO) pavement performance model is widely used for design and evaluation of flexible pavements in the United States (1). This model is a result of statistical analyses of performance data obtained from the carefully designed experimental pavements at the AASHO test road. Because the data base used for the model development is related specifically only to soil and pavement materials, construction procedures, loading conditions, and environmental conditions that existed at the AASHO Road Test, the AASHO Committee on Design called for satellite studies to extend AASHO Road Test results to various environments, traffic, and construction practices (2).

The Pennsylvania Transportation Research Facility, which was constructed by using Pennsylvania's construction practices, is located near the geographical center of the Commonwealth so that the environmental conditions can be considered as representative of the entire state. Therefore, the study at the Research Facility serves the purpose to extend AASHO test results to the conditions present in Pennsylvania, although it is not the sole objective of the research. This paper presents the results of performance analyses for the experimental pavements at the Research Facility. Meanwhile, some existing pavement performance models are compared, and various equations that permit prediction of pavement performance from response variables are presented.

PENNSYLVANIA TRANSPORTATION RESEARCH FACILITY

The Pennsylvania Transportation Research Facility is a one-mile, one-lane test road. The original facility was constructed in summer 1972 and was composed of 17 test pavements of various lengths. Each pavement contained either different base-course materials with the same layer thickness or one type of base-ccurse material with different layer thicknesses, as shown in Figure 1. Of these pavement sections, section 8 was overlaid and sections 10 through 12 were replaced by eight shorter sections in fall 1975. All pavements were 12 ft wide.

The subgrade soil was a silty clay that had classifications that ranged from A-4 to A-7 according to the AASHO classification and CL according to the Unified Soil Classification. The subbase material was a crushed limestone. The base-course materials were bituminous concrete, aggregate cement, aggregate-lime-pozzolan, aggregate bituminous, and crushed stone. In the aggregate-cement base course, three types of aggregate were used--limestone, slag, and gravel. Of the aggregate-lime-pozzolan pavements, sections F and G were excluded from the analysis because they were unable to cure properly due to cold weather during construction. The wearing surface was an ID-2A bituminous concrete.

The traffic on the Research Facility was provided by a conventional truck tractor pulling a semitrailer and one or two full trailers. Scrap steel was used as the lading on the test vehicle. A total of about 2.4 million and 1.3 million applications of 18-kip equivalent axle load (EAL_{18}) had been applied to the pavements constructed in 1972 and 1975, respectively. Complete information on design, construction, and traffic operation is documented elsewhere (3,4).

MATERIAL PROPERTIES

The composition, gradation, and index properties of the constituent material of each pavement are documented in a research report (3). The modulus of elasticity of each layer was determined by using laboratory repeated-load tests on laboratory-compacted test specimens. The specimens had a diameter of 6 in and a height of 10 in. The repeated load had a frequency of 20 cycles/min and a duration of 0.1 s. The modulus values obtained for the spring weather conditions are summarized in Table 1. In the spring season, the average pavement temperature was approximately 60°F, and the average subgrade moisture content was about 23 percent. Also given in Table 1 is Poisson's ratio for each pavement constituent material. These data are obtained from other studies (5-7). Other material properties such as fatigue and viscoelastic properties are available elsewhere (8). They are not used in this paper and therefore are not included in Table 1.

The structural coefficients of the pavement materials are also included in Table 1. Of these values, the structural coefficients of the surface and subbase materials are obtained from the AASHO Interim Guide (1,2). The structural coefficients of the base-course materials are determined by using two different methods of analysis--the AASHO performance analysis and the limiting criteria approach. The first analysis was based on the use of performance data with analysis techniques similar to those used at the AASHO Road Test. The second approach was based on the limiting criteria so that the pavement deflection, maximum tensile strain at the bottom of the stabilized base, and maximum compressive strain at the top of the subgrade can be limited within permissible values. Detailed analyses are available elsewhere (9).

FIELD EVALUATION AND TESTING

Field evaluation of pavement performance was conducted periodically. Rut depth was measured biweekly every 40 ft in both wheel paths by using an A-frame that was attached to a 7-ft-long base channel. Surface cracking was surveyed and mapped biweekly. Surface roughness was measured in both wheel paths by using a MacBeth profilograph. The roughness factors obtained from the profilograph data were converted into present serviceability index (PSI) of the pavement by using the following equations:

$$PSI = 11.33 - 4.06 (\log RF) - 0.01\sqrt{C + P} - 0.21\ \overline{RD}^2 \quad (1)$$

$$RF = 63.267 + 0.686\ R \quad (2)$$

where

RF = Mays meter roughness factor,
C = area of cracking (ft²/1000 ft²),
P = area of patching (ft²/1000 ft²),
$\overline{RD}$ = average rut depth (in), and
R = profilograph readings (in/mile).

These two equations were developed by Hopkins (10) of the Pennsylvania Department of Transportation (PennDOT).

In addition, surface deflections were measured in the wheel paths by using the Benkelman beam and the

Figure 1. Plan view and longitudinal profile of test track.

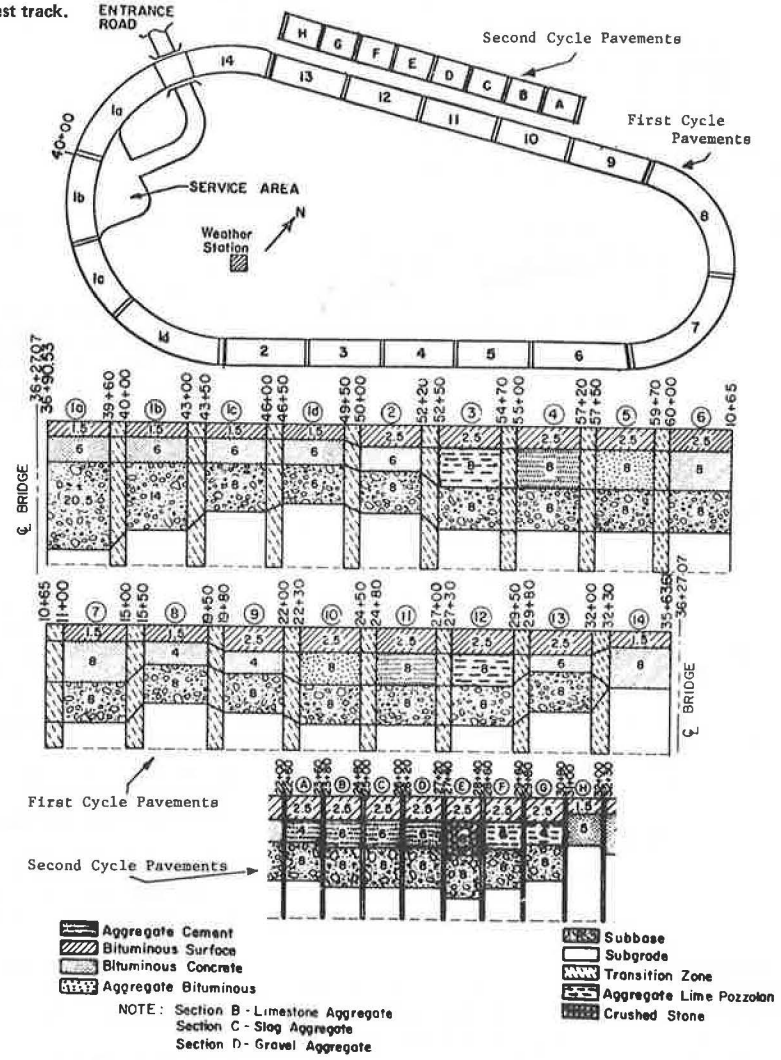

Table 1. Elastic constants and structural coefficients of pavement constituent materials for spring weather conditions.

Layer	Material	Elastic Modulus (psi 000s)	Poisson's Ratio	Structural Coefficient[a]	
				H_1 = 1.5 in	H_1 = 2.5 in
Surface	Bituminous concrete	140	0.40	0.44	0.44
Base	Bituminous concrete	320	0.35	0.35	0.32
	Limestone aggregate cement	3600	0.20	0.35	0.28
	Slag aggregate cement	3200	0.20	0.23	0.19
	Gravel aggregate cement	2500	0.20	0.21	0.17
	Aggregate-lime-pozzolan	2400	0.15	0.24	0.21
	Aggregate bituminous	100	0.35	0.26	0.24
Subbase	Crushed limestone	48	0.40	0.11	0.11
Subgrade	Silty clay	8	0.45	-	-

[a] H_1 = thickness of surface layer.

Table 2. PSI data.

Section No.	Base-Course Material[a]	Layer Thickness (in)			Structural No. (SN)	Initial PSI (PSI_o)	β	EAL (10^6) at ΔPSI =			
		Surface	Base	Subbase				0.5	1.0	1.5	2.0
1b	BC	1.5	6	14	4.30	3.35	1.36	2.04	-	-	-
1c	BC	1.5	6	8	3.64	3.45	1.95	1.74	2.70	-	-
1d	BC	1.5	6	6	3.42	3.50	1.54	1.07	2.02	2.37	2.54
2	BC	2.5	6	8	3.90	3.50	2.01	2.40	-	-	-
3	ALP	2.5	8	8	3.66	3.90	1.85	1.38	1.76	1.99	2.18
4	AC	2.5	8	8	5.98	3.85	0.95	-	-	-	-
5	AB	2.5	8	8	3.90	3.75	1.51	1.55	2.11	2.35	2.46
6	BC	2.5	8	8	4.38	3.30	1.30	2.29	-	-	-
7	BC	1.5	8	8	4.34	3.55	1.25	1.52	2.62	-	-
8	BC	1.5	4	8	2.94	3.30	2.10	0.52	0.79	1.02	1.18
9	BC	2.5	4	8	3.26	3.80	1.68	0.73	1.08	1.35	1.50
A	AC	2.5	4	8	3.18	3.75	2.13	0.63	0.92	1.10	1.21
B	AC	2.5	6	8	3.66	3.75	1.97	0.97	1.33	-	-
C	AC	2.5	6	8	3.12	3.85	2.57	0.84	1.07	1.22	1.32
D	AC	2.5	6	8	3.00	3.70	2.66	0.61	0.80	1.02	1.13
E	CS	2.5	8	8	2.86	3.70	2.25	0.28	0.49	0.64	0.77
H	BC	1.5	5	0	2.41	3.25	3.20	0.26	0.32	0.36	0.38
14	BC	1.5	8	0	3.46	3.20	1.80	0.83	1.26	1.55	-

[a]Base-course materials: BC = bituminous concrete, AC = aggregate cement, ALP = aggregate-lime-pozzolan, AB = aggregate bituminous, and CS = crushed stone.

Figure 2. Serviceability data and comparison of various models.

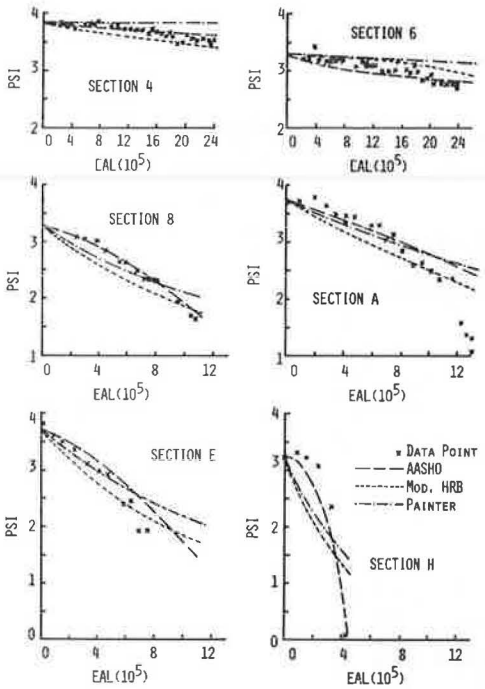

road rater. Pavement temperature profile and subgrade moisture distribution were measured by using thermocouples and moisture cells. Also, two frost-depth indicators were installed at the Research Facility to measure the depth of frost penetration. Weather data such as wind velocity, precipitation, and temperature were collected by using various meteorological gages.

PRESENT SERVICEABILITY INDEX

The complete record of PSI data for the test pavements is documented in a research report (11). Table 2 summarizes the initial PSI values and the number of 18-kip EALs required for various levels of PSI drop for all pavements except sections 1A, F, and G. These three sections are excluded because section 1A was overloaded by the equipment used for bridge construction and both sections F and G were not properly cured, as mentioned earlier. The variation of PSI with EAL for two thick pavements (sections 4 and 6), two thin pavements (sections 8 and A), one pavement with a crushed-stone base (section E), and one thin full-depth bituminous pavement (section H) is shown in Figure 2. Both Figure 2 and Table 2 demonstrate that the initial PSI values are generally low (compared with those at the AASHO test road) and vary considerably between each pavement.

Figure 2 also indicates that the serviceability loss can be described by the same power function of axle-load applications as that used at the AASHO Road Test (12):

$$c_o - P = (c_o - c_1)(W/\rho)^{\beta} \quad (3)$$

where

c_o = initial PSI,
c_1 = terminal serviceability index,
P = PSI at time t,
W = number of EALs at time t,
ρ = pavement life expressed in terms of EAL, and
β = rate of change of serviceability loss.

By fitting the power function (Equation 3) to the observed PSI versus EAL data, the two indicators of pavement performance (β and ρ) are obtained and tabulated in Table 2. Note that because of the considerable variation in the initial PSI values, the ρ values are estimated for various levels of PSI drop rather than for fixed values of terminal serviceability index. Also included in Table 2 are the type of base-course material, layer thickness, and structural number (SN) of each pavement section. SN is computed as follows:

$$SN = a_1H_1 + a_2H_2 + a_3H_3 \quad (4)$$

where H_1, H_2, and H_3 are the layer thickness (in inches) of the surface, base, and subbase, respectively; and a_1, a_2, and a_3 are the structural coefficients of the surface, base, and subbase, respectively. The structural coefficient values are obtained from Table 1.

The effect of SN on the PSI versus EAL relation can be described by available mathematical models such as the AASHO performance model (2), modified Highway Research Board (HRB) model (13), and Painter's model (14). The AASHO model is given by the following equation:

$$G/\beta = \log (EAL) - 9.36 \log (SN + 1) + \log R - 0.372 (S - 3.0) + 0.20 \quad (5)$$

where

$G = \log [(PSI_o - PSI)/(PSI_o - 1.5)]$, (5a)

PSI_o = initial PSI value,

$\beta = 0.40 + 1094(SN + 1)^{-5.19}$, (5b)

S = soil support value, and

R = regional factor.

Table 1 indicates that the subgrade soil at the Research Facility has a resilient modulus of 8000 psi. The soil support value that corresponds to this resilient modulus value is about 5.5 according to Van Til and others (1). The temperature and precipitation data at the Research Facility suggest a regional factor of 1.5. Incorporating these two values into Equation 5 yields the following equation:

$$G/\beta = \log (EAL) - 9.36 \log (SN + 1) - 0.554 \quad (6)$$

The PSI values predicted by using Equations 5a, 5b, and 6 are compared with the observed data in Figure 2. The comparison indicates that the prediction is quite good in the early stage of the pavement life. As the pavement becomes older, however, the AASHO model overpredicts pavement performance. This is in agreement with the recent findings of Darter (15).

The modified HRB performance model for flexible pavement is as follows:

$$\log (PSI_o/PSI) = EAL/[4D^8 (RS)^4] \quad (7)$$

where

$D = 0.54H_1 + 0.16r_2H_2 + 0.14H_3 + 1.00$, (7a)

r_2 = constant whose value depends on the type of base-course material, and

RS = relative strength that is used to consider the effect of regional factor; a factor of 1.5 is used in this analysis.

Painter's model relates PSI with EAL through the following equation:

$$\log (PSI_o/PSI) = F (EAL \times 10^{-6})/\log^{-1} D \quad (8)$$

where

$D = a_1H_1 + a_2H_2 + a_3H_3 - 1.52$, (8a)

and F is environmental factor; a value of 6 is used in this analysis. The predicted pavement performance by using the modified HRB and Painter's models is also shown in Figure 2. It is seen that Painter's model overpredicts performance more than the modified HRB model. Of the three performance models analyzed, the AASHO model appears to predict best, although it also overpredicts performance at the later stage of pavement life.

To improve the AASHO performance model, the pavement performance indicator (β value), which is tabulated in Table 2, is correlated with SN for all of the pavements analyzed. As shown in Figure 3, the correlation is well defined. From this correlation, the following equation is obtained:

$$\beta = 0.12 + 31.62 (SN + 1)^{-1.92} \quad (9)$$

The number of EALs (in millions) required for various levels of PSI drop (ΔPSI) tabulated in Table 2 is also correlated in Figure 4. The values of r^2 range from 0.88 to 0.95. These correlations give the following equations. For $\Delta PSI = 0.5$,

$$EAL = 2.94 \times 10^{-4} (SN + 1)^{5.42} \quad (10)$$

For $\Delta PSI = 1.0$,

$$EAL = 3.78 \times 10^{-4} (SN + 1)^{5.45} \quad (11)$$

For $\Delta PSI = 1.5$,

$$EAL = 2.23 \times 10^{-4} (SN + 1)^{6.02} \quad (12)$$

And for $\Delta PSI = 2.0$,

$$EAL = 1.06 \times 10^{-4} (SN + 1)^{6.67} \quad (13)$$

By using Equations 10 through 13, it will be possible to predict the number of EALs (in millions) required to produce a certain level of PSI drop for a given SN value. Conversely, the value of SN required to withstand a predetermined EAL can also be determined. For example, to limit PSI drop at 2 million EALs within 0.5, 1.0, 1.5, and 2.0, the pavement must have SN values of at least 4.1, 3.8, 3.5, and 3.4, respectively.

ROUGHNESS, RUTTING, AND CRACKING

Three major modes of distress manifestation are longitudinal roughness, transverse rutting, and surface cracking. Cracking can be caused by loading, thermal stress, settlement, heaving, etc. However, only load-associated cracking is treated here. Table 3 summarizes roughness, rutting, and cracking data. From these data, relations between SN and each distress manifestation are established. These relations permit prediction of either the maximum EAL to produce certain levels of distress in a given pavement or the minimum SN value so that at certain EAL the distress will not exceed a predetermined level.

Figure 5 shows the relations between SN and EAL to cause two levels of roughness, namely, 10 and 30

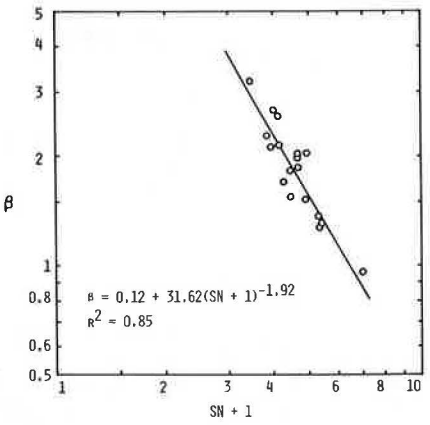

Figure 3. Pavement performance indicator (β) versus (SN + 1).

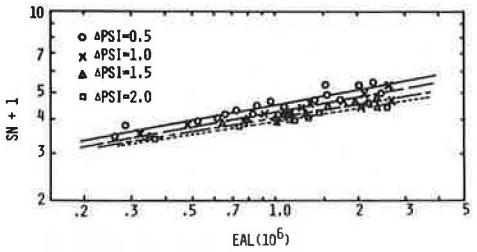

Figure 4. (SN + 1) versus EAL for four levels of PSI drop.

Table 3. Roughness, rut depth, and cracking data.

Section No.	SN	EAL (10^6) at R (in/mile) =			EAL (10^6) at RD (in) =			EAL (10^6) at C (ft^2/1000 ft^2) =		
		10	20	30	0.25	0.50	0.75	10	60	100
1b	4.30	0.92	1.80	-	1.69	-	-	-	-	-
1c	3.64	0.60	1.45	-	1.45	-	-	-	-	-
1d	3.42	0.51	1.03	1.56	1.14	1.82	2.39	1.80	-	-
2	3.90	1.10	-	-	1.68	-	-	-	-	-
3	3.66	0.70	1.29	1.58	1.41	1.93	2.27	1.26	1.80	2.15
4	5.98	1.53	-	-	2.33	-	-	-	-	-
5	3.90	0.40	0.64	0.78	1.12	1.89	2.34	2.40	-	-
6	4.38	1.54	-	-	1.60	2.53	-	-	-	-
7	4.34	0.52	1.11	1.92	1.49	2.47	-	-	-	-
8	2.94	0.13	0.27	0.40	0.63	0.95	1.17	0.39	0.98	-
9	3.26	0.23	0.49	0.82	0.56	1.02	1.40	1.04	1.31	1.46
A	3.18	0.40	0.64	0.78	0.76	1.12	1.31	1.13	1.22	-
B	3.66	0.69	0.95	1.14	1.72	-	-	-	-	-
C	3.12	0.65	0.88	1.02	0.88	1.21	1.39	1.21	1.27	1.30
D	3.00	0.47	0.65	0.76	0.80	1.14	1.26	0.75	1.20	1.23
E	2.86	0.15	0.35	0.52	0.18	0.49	0.74	0.61	0.65	0.66
H	2.41	0.13	0.21	0.27	0.29	0.32	0.35	0.36	-	-
14	3.46	0.16	0.33	0.50	1.20	1.61	-	1.00	1.35	1.50

Figure 5. (SN + 1) versus EAL for two levels of roughness.

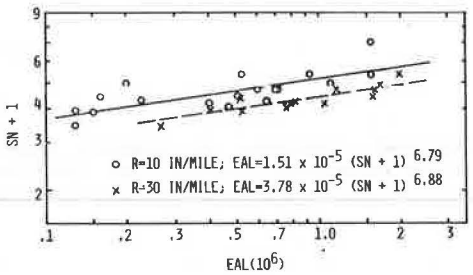

Figure 6. (SN + 1) versus EAL for three levels of rutting.

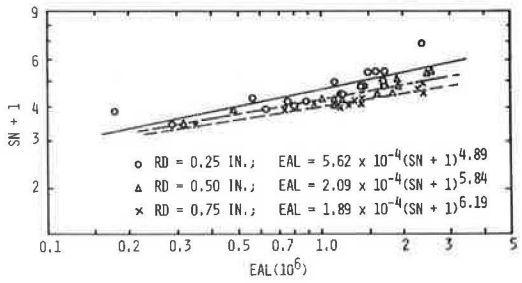

in/mile. Data points are somewhat scattered, but the trend is very clear. The values of r^2 are 0.83 and 0.90 for 10 and 30 in/mile, respectively. Equations for the two relations are given in the figure. The data indicate that, for a pavement with an SN equal to 3.5, roughness will reach 10 and 30 in/mile at an EAL of about 0.86 and 2.5 millions, respectively. Also, for a pavement to withstand 2.0 million EALs without roughness exceeding 10 and 30 in/mile, the minimum values of SN required will be about 4.6 and 3.9, respectively.

The relations between SN and EAL to cause three levels of rutting are shown in Figure 6. Equations that relate SN and EAL are given in the figure. According to this figure, for a pavement that has an SN equal to 3.5, the amount of rutting will reach 0.25, 0.50, and 0.75 in at EALs of about 0.9, 1.4, and 2.1 millions, respectively. Further, the minimum values of SN for pavements to withstand 2.0 million EALs with maximum rutting of 0.25, 0.50, and 0.75 in are about 4.4, 3.9, and 3.5, respectively.

Figure 7. (SN + 1) versus EAL for two levels of surface cracking.

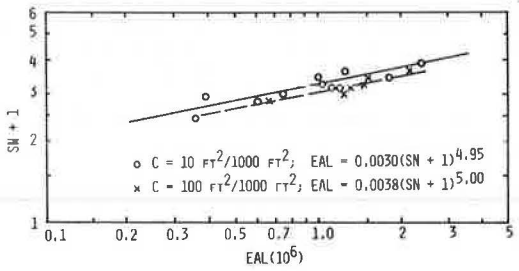

Figure 7 relates the SN and EAL required to cause two levels of cracking intensity--10 and 100 ft^2/1000 ft^2. From this relation, to limit cracking intensity within 100 ft^2/1000 ft^2 at the end of 2.0 million EALs, the SN of the pavement must be at least 2.5. For this SN value, surface cracking of 10 ft^2/1000 ft^2 will develop at EAL of about 1.5 million.

PAVEMENT RESPONSE

Critical response data, including maximum surface deflection, maximum compressive strain at the top of the subgrade, and maximum tensile strain at the bottom of the stabilized layer, are tabulated in Table 4. These critical response data were obtained from an analysis that was made by using an elastic-layer computer program together with the elastic properties tabulated in Table 1. The computer program used was the Bitumen Structures Analysis in Roads (BISAR) that was developed at Koninklijke/Shell Laboratorium in Amsterdam, The Netherlands. The traffic loading used in the analysis was an 18-kip EAL on dual wheels that had a tire pressure of 80 lbf/in^2.

The initial maximum surface deflections analyzed are in good agreement with the measured maximum Benkelman beam deflections. These deflection data are correlated with SN values in Figure 8. Two distinct relations result: one for pavements that contain bituminous concrete, crushed stone, and aggregate bituminous base, and the other for pavements with aggregate cement and aggregate-lime-pozzolan base. The r^2-value of the correlation for the aggregate cement and aggregate-lime-pozzolan pavements is 0.80 and that for the other pavements is 0.92. For a given value of SN, the deflection is

Table 4. Maximum deflection, compressive subgrade strain, and tensile strain data.

Section No.	SN	Initial Maximum Deflection (10^{-3} in)	Maximum Compressive Strain (10^{-6})	Maximum Tensile Strain (10^{-6})
1b	4.30	15.8	294.2	85.1
1c	3.64	23.0	426.6	100.2
1d	3.42	28.0	483.0	109.5
2	3.90	21.5	383.6	89.6
3	3.66	9.0	142.8	41.1
4	5.98	6.5	107.5	28.5
5	3.90	21.0	403.0	165.0
6	4.38	15.0	291.6	70.9
7	4.34	19.0	322.4	84.6
8	2.94	39.0	594.0	139.0
9	3.26	29.0	525.8	122.7
A	3.18	14.0	288.0	65.0
B	3.66	7.5	171.5	42.2
C	3.12	15.0	185.5	46.1
D	3.00	15.0	216.0	54.4
E	2.86	31.0	575.4	279.4[a]
H	2.41	40.0	844.8	209.1
14	3.46	35.0	390.9	118.1

[a]For section E, which has a crushed-stone base, maximum tensile strain at bottom of the surface layer is used.

Figure 8. Maximum surface deflection versus (SN + 1).

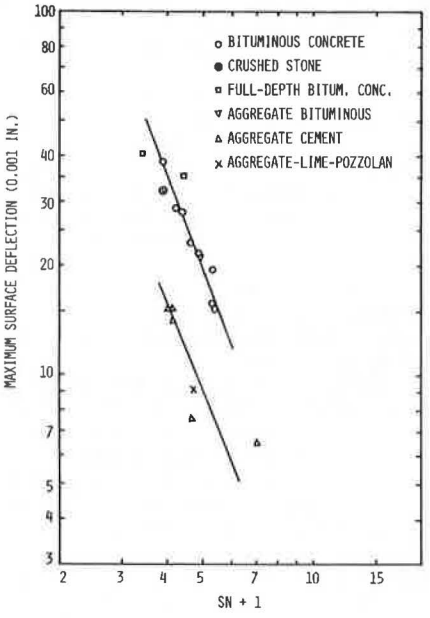

smaller for aggregate cement and aggregate-lime-pozzolan pavements than the other pavements. This is as would be expected, since aggregate cement and aggregate-lime-pozzolan have higher moduli than the other base-course materials, as shown in Table 1. Under the same intensity of loading, surface deflection decreases with increasing layer modulus value.

According to the relations in Figure 8, maximum surface deflection can be related with SN by the following equations. For pavements that contain bituminous concrete, crushed stone, and aggregate-bituminous base,

$$\delta = 0.85 + 1287.30\,(SN + 1)^{-2.58} \quad (14)$$

And for pavements with aggregate cement and aggregate-lime-pozzolan base,

$$\delta = 0.24 + 544.80\,(SN + 1)^{-2.58} \quad (15)$$

where δ is the maximum surface deflection (0.001 in). Equations 14 and 15 may be combined with Equations 10 through 13 to form relations between maximum surface deflections and EAL (in millions) required to cause predetermined PSI drops. These equations are as follows. For $\Delta PSI = 0.5$,

Bituminous concrete pavements: $EAL = 996.95\,(\delta + 0.85)^{-2.10}$ (16)

Aggregate cement pavements: $EAL = 163.85\,(\delta - 0.24)^{-2.10}$ (16a)

For $\Delta PSI = 1.0$,

Bituminous concrete pavements: $EAL = 1377.05\,(\delta + 0.85)^{-2.11}$ (17)

Aggregate cement pavements: $EAL = 224.36\,(\delta - 0.24)^{-2.11}$ (17a)

For $\Delta PSI = 1.5$,

Bituminous concrete pavements: $EAL = 3925.18\,(\delta + 0.85)^{-2.33}$ (18)

Aggregate cement pavements: $EAL = 529.34\,(\delta - 0.24)^{-2.33}$ (18a)

And for $\Delta PSI = 2.0$,

Bituminous concrete pavements: $EAL = 12\,005.39\,(\delta + 0.85)^{-2.59}$ (19)

Aggregate cement pavements: $EAL = 1294.67\,(\delta - 0.24)^{-2.59}$ (19a)

By using Equations 16 through 19a, it would be possible to estimate the EAL required to cause various levels of PSI drop for flexible pavements with different base-course materials.

The maximum strain data in Table 4 are correlated with SN in Figures 9 (compressive strain) and 10 (tensile strain). It is seen that the correlation for maximum compressive strain is much better than that for maximum tensile strain. The r^2-values for compressive strain correlations are 0.96 and 0.82 for bituminous concrete pavements and aggregate cement pavements, respectively. The equations of the correlations are as follows. For pavements with bituminous concrete, crushed stone, and aggregate-bituminous base,

$$\epsilon_v = 14.81 + 14\,805.05\,(SN + 1)^{-2.305} \quad (20)$$

And for pavements with aggregate cement and aggregate-lime-pozzolan base,

$$\epsilon_v = 5.50 + 3318.0\,(SN + 1)^{-1.875} \quad (20a)$$

In Equations 20 and 20a, ϵ_v is the maximum compressive strain (in millionths).

A comparison of Figure 8 with Figure 9 indicates that the correlation between the maximum compressive strain and SN is slightly better than the surface deflection versus SN correlation. By combining Equations 20 and 20a with Equations 10 through 13, relations between compressive strain and EAL will result. These relations permit prediction of EAL for various levels of ΔPSI from known compressive strains. It is interesting to note that Luhr and McCullough (16) also found that compressive strain gives a slightly better prediction of pavement performance. Although the maximum compressive strain is a better performance predictor than the maximum deflection, the use of the predicting equations usually requires an elastic-layer analysis to obtain compressive strain as input data. When only surface deflection data are available, it is more convenient to use Equations 16 through 19 to estimate pavement performance.

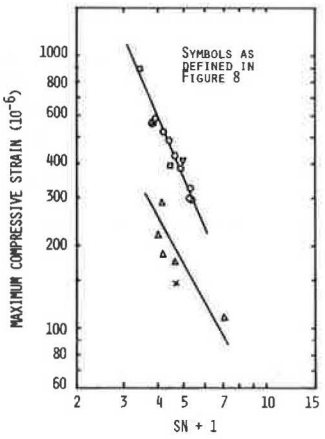

Figure 9. Maximum compressive strain at top of subgrade versus (SN + 1).

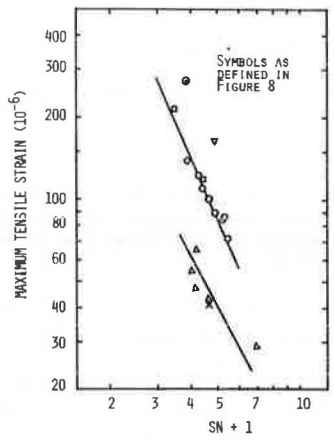

Figure 10. Maximum tensile strain at bottom of stabilized base versus (SN + 1).

SUMMARY AND CONCLUSIONS

The performance of experimental pavements at the Pennsylvania Transportation Research Facility was evaluated. Data analyzed were pavement serviceability index and three distress manifestations--roughness, rutting, and cracking. Some existing pavement performance models were evaluated by using the performance data; those evaluated were AASHO, modified HRB, and Painter's models.

The performance data indicate that the trend of serviceability index loss with increasing EAL follows the power function developed at the AASHO Road Test. Of the three performance models evaluated, the AASHO model appears to predict best, although it overpredicts pavement service life. By using a curve-fitting process and regression analysis, equations that relate pavement performance with SN, distress with SN, and performance with critical response are developed. These equations may be used to predict pavement performance from SN or critical pavement response.

ACKNOWLEDGMENT

The paper presented here is a part of the research project, A Study of Flexible Pavement Base Courses and Overlay Designs, sponsored by PennDOT in cooperation with the Federal Highway Administration (FHWA), U.S. Department of Transportation. Their support is gratefully acknowledged. The field data reported here were collected and reduced with the assistance of W.P. Kilareski, S.A. Kutz, B.A. Anani, R.P. Anderson, P.J. Kersavage, and Johannes Karundeng. This paper represents my views and does not necessarily reflect those of PennDOT or FHWA.

REFERENCES

1. C.J. Van Til, B.F. McCullough, B.A. Vallerga, and R.G. Hicks. Evaluation of AASHO Interim Guides for Design of Pavement Structures. NCHRP, Rept. 128, 1972.
2. AASHO Interim Guide for Design of Pavement Structures, 1972. AASHO, Washington, DC, 1972.
3. E.S. Lindow, W.P. Kilareski, G.Q. Bass, and T.D. Larson. Construction, Instrumentation, and Operation: Vol. 2, Interim Report on an Evaluation of Pennsylvania's Flexible Pavement Design Methodology. Pennsylvania Transportation Institute, Pennsylvania State Univ., University Park, Rept. PTI 7504, Feb. 1973.
4. W.P. Kilareski, S.A. Kutz, and G. Cumberledge. Modification, Construction, and Instrumentation of an Experimental Highway, Interim Report on a Study of Flexible Pavement Base Course and Overlay Design. Pennsylvania Transportation Institute, Pennsylvania State Univ., University Park, Rept. PTI 7607, April 1976.
5. K. Nair, W.S. Smith, and C.Y. Chang. Characterization of Asphalt Concrete and Cement-Treated Granular Base Course, Final Report. FHWA, Feb. 1972.
6. S. Kolis and R.I.T. Williams. Cement-Bound Road Materials: Strength and Elastic Properties Measured in the Laboratory. Transport and Road Research Laboratory, Crowthorne, Berkshire, England, TRRL Supplementary Rept. 334, 1978.
7. Lime-Fly Ash-Stabilized Bases and Subbases. NCHRP, Synthesis of Highway Practice 37, 1976.
8. M.G. Sharma and T.D. Larson. The Pennsylvania Pavement Research Facility: Vol. 4, Mechanical Characterization of Materials. Pennsylvania Transportation Institute, Pennsylvania State Univ., University Park, Interim Rept. PTI 7509, Aug. 1974.
9. M.C. Wang and T.D. Larson. Evaluation of Structural Coefficients of Stabilized Base-Course Materials. TRB, Transportation Research Record 725, 1979, pp. 58-67.
10. J.G. Hopkins. Pavement Roughness and Serviceability, Final Report. Bureau of Materials, Testing, and Research, Pennsylvania Department of Transportation, Harrisburg, Aug. 1975.
11. W.P. Kilareski, B. Anani, R.P. Anderson, M.C. Wang, and T.D. Larson. Remaining Life and Overlay Thickness Design for Modified Flexible Pavements. Pennsylvania Transportation Institute, Pennsylvania State Univ., University Park, Interim Rept. PTI 7905, Jan. 1979.
12. The AASHO Road Test: Report 5, Pavement Research. HRB, Special Rept. 61E, 1962.
13. P.E. Irick and W.R. Hudson. Guidelines for Satellite Studies of Pavement Performance. NCHRP, Rept. 2A, 1964.
14. L.J. Painter. Analysis of AASHO Road Test Data by the Asphalt Institute. Proc., International Conference on Structural Design of Asphalt Pavements, Univ. of Michigan, Ann Arbor, 1962, pp. 84-97.
15. M.I. Darter. Requirements for Reliable Predictive Pavement Models. TRB, Transportation Research Record 766, 1980, pp. 25-31.
16. D.R. Luhr and B.F. McCullough. Development of a Rationally Based AASHO Road Test Algorithm. TRB, Transportation Research Record 766, 1980, pp. 10-17.

Publication of this paper sponsored by Committee on Flexible Pavement Design.